Effect of Organoclay Reinforcement on the Curing Characteristics and Technological Properties of SBR Sulphur Vulcanizates

J. Diez,[1] R. Bellas,[1] C. Ramírez,[1] A. Rodríguez[2]

[1]*Departamento de Física, E.U.P., Ferrol, Universidad de A Coruña, Ferrol 15405, Spain*
[2]*Departamento de Química y Tecnología de Elastómeros, Instituto de Ciencia y Tecnología de Polímeros, CSIC, Madrid 28006, Spain*

Received 21 September 2009; accepted 5 March 2010
DOI 10.1002/app.32431
Published online 21 May 2010 in Wiley InterScience (www.interscience.wiley.com).

ABSTRACT: Styrene-butadiene rubber (SBR) nanocomposites with different organoclay contents (up to 15 phr) were prepared by a melt compounding procedure, followed by a compression-molding step in which the SBR matrix was sulfur crosslinked. The vulcanizates were characterized in respect to their curing, mechanical and viscoelastic properties, and thermal stability. The optimum cure time decreased with increasing organoclay content. This effect was attributed to the ammonium modifier present in the organoclay, which takes part in the curing reaction acting like an accelerator. The results of mechanical test on the vulcanizates showed that the nanocomposites presented better mechanical properties than unfilled SBR vulcanizate, indicating the nanoreinforcement effect of clay on the mechanical properties of SBR/organoclay nanocomposites. The addition of organoclay did not significantly change the glass transition temperature. However, the heights of tan δ value at the glass transition temperature for the nanocomposites are lower than that of the unfilled SBR. This suggests a strong interaction between the organoclay and the SBR matrix as the molecular relaxation of the latter is hampered. The temperature at which 50% degradation occurs (T_{50}) and the temperature when the degradation rate is maximum (DTG_{max}) showed an improvement in thermal stability, probably related to the uniform dispersion of organoclay. © 2010 Wiley Periodicals, Inc. J Appl Polym Sci 118: 566–573, 2010

Key words: styrene-butadiene rubber; nanocomposites; reinforcement; mechanical properties

INTRODUCTION

Styrene-butadiene rubber (SBR) is one of the most widely employed synthetic rubbers. This polymer is mainly used in the manufacture of tyres but it is employed in many other industrial applications such as membranes, shoe soling, pharmaceutical, and sanitary products, etc. Due to the continuous demand for new materials, SBR needs reinforcement to satisfy the stringent industrial requirements. A wide range of particulate fillers is incorporated into the rubber matrices mainly to improve and modify the physicomechanical properties rubber matrices and in many cases to reduce the material cost. Carbon black and silica are usually used to reinforce vulcanized rubbers. However, a minimum of 20 phr of filler content is usually needed for a significant property enhancement. Nowadays, there is a great scientific and industrial interest in the development of rubber nanocomposites with layered silicates as reinforcements as an alternative to conventional highly filled rubber compounds.[1,2] Nanocomposites exhibit new and improved performance properties when compared with pristine rubber,[3] even when they are prepared with a very small amount of layered silicate (less than 10 phr). The basic principle of rubber clay nanocomposite formation is that the rubber should penetrate into the intergalleries of the clay, so the space between the platelets or layered galleries of the silicate should be made accessible for the rubber chains. This occurs by replacing the original small cations by more bulky organic molecules increasing the initial interlayer distance and making the silicate surface organophilic. The resulting organoclay can well be dispersed in the polymer. The aim of this work was to study the effect of a commercial organophilic nanosilicate on the curing, tensile, viscoelastic, and thermal properties of a SBR.

Correspondence to: J. Diez (jdiez@udc.es).
Contract grant sponsor: Consellería de Educación, Xunta de Galicia (Axudas do Programa de Consolidación Expte); contract grant number: 2007/0008_0.

EXPERIMENTAL

Materials

SBR 1502, supplied by Dow Chemical, was used in this work. The organoclay used as filler was a

TABLE I
Composition of Organoclay Filled SBR Composites

Ingredients	Phr[a]
SBR 1502	100
Estearic acid	1
Zinc oxide	5
2-Mercaptobenzothiazole	1
Sulphur	3
Organoclay	0–15

[a] Parts per hundred of rubber by weight.

montmorillonite modified by octadecylamine (Nanomer® I.30E, Nanocor Inc.).

Other curing additives (ZnO, stearic acid, 2-mercaptobenzothiazole (MBTS) and sulfur were of analytical grade.

Compounding

Mixing was performed in a 50 mL internal mixer Brabender Plasticorder PLE2000 at a set temperature of 60°C with a rotor speed at 60 rpm. The fill factor (the ratio of the charged rubber compound to mixer capacity) was 0.8. A rubber standard was prepared without clay. Rubber/organoclay composites were prepared at four different clay concentrations (2.5, 5, 10, and 15 phr). Brabender Mixing Software 3.2.11 was used for controlling mixing conditions and storing data. The formulations of rubber compounds are given in Table I.

Compounding was carried out in two steps to avoid the increase of temperature and the scorch of the mixtures during mixing. In the first step, SBR, filler, stearic acid, and zinc oxide were mixed for 14 min. Then, the compounds were dumped and left at ambient temperature to cool down to about 45–50°C. Subsequently, the compound were reintroduced in the chamber and premixed for 1 min. Then, MBTS and Sulphur were added. As a representative example, the different mixing intervals can be observed from torque-time graphs (Fig. 1).

The vulcanizate sheets were obtained by compression molding using an electrically heated hydraulic press at 160°C for the optimum cure time determined as t_{97} by rheometry under a pressure of 20 MPa.

Cure time determination

The cure characteristics were determined at 160°C using a Monsanto Moving Die Rheometer, MDR2000E, at 1.66 Hz frequency and 0.5 arc, as per ISO 6502:1999.

Structure characterization

X-ray diffraction (XRD) was used to characterize the nature and extent of the dispersion of the organoclay in the filled samples. XRD were collected using a Siemens D5000 diffractometer at the wavelength Cu Kα = 1.54 Å, a tube voltage of 40 kV and a tube current of 25 mA. Bragg's law defined as $n\lambda = 2d \sin \theta$, was used to compute the crystallographic spacing (d) for the organoclay. The samples were scanned in the range of 1.15–10°.

The dispersion and morphology of the clay particles in the composites was studied by transmission electron microscopy (TEM). Samples were produced using an ultracryomicrotome and they were examined with a JEOL 1010 TEM with an acceleration voltage of 80 kV.

Physical and mechanical properties

1. The tensile properties (elongation at break, modulus at 100% elongation (M100) and tensile strength at break) of the rubber vulcanizates were measured using an Instron 5566 Universal Test machine according to ASTM D638-2003. Dumbell-shaped specimens (Type IV) were analyzed at room temperature with a crosshead speed of 50 mm/min.

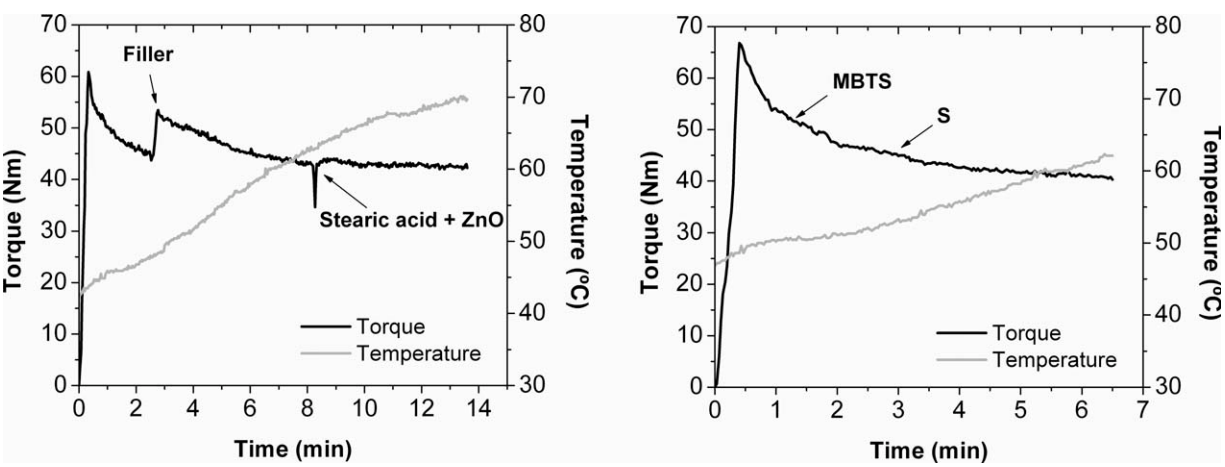

Figure 1 Mixing torque-time graphs of the SBR vulcanizate loading with 10 phr organoclay.

2. The tear strength was determined according to ISO 34-1:1994. Unnicked angle test pieces were tested using an Instron 5566 Universal Test machine at room temperature with a crosshead speed of 50 mm/min at room temperature.
3. The resilience measurements were carried out by rebound test according to ISO 4662 : 1986 specification on a Schob pendulum at room temperature.
4. The compression set was assessed according to ISO 3384 : 1999 at a test temperature of 70°C for 24 h. Standard test specimens of cylindrical shape with 20 mm diameter and 15 mm thickness were used and the percentage of compression employed was 25% of the samples original thickness.
5. Shore A hardness was measured by using a Hampden M202 durometer according to ISO 868–2003 test method.
6. The dynamomechanical analysis was carried out using a Perkin Elmer DMA 7 dynamomechanical analyzer using circular samples of 10 mm diameter and 3 mm thickness and parallel plate geometry. Testing was performed in the temperature scan mode heating from −70 to 70°C at a rate of 2°C/min and 1 Hz of frequency.
7. Thermal degradation measurements were carried out on Perkin Elmer TGA 7 thermobalance at a heating rate of 10°C/min under argon atmosphere.

Thermal aging

The effect of thermal aging on the property changes of the SBR filled with organoclay was studied using the standard method ISO 168–2007. The vulcanizates underwent thermooxidative aging, conducted in an air-circulating oven at 70°C for 3 and 7 days. Shore A hardness and the tensile properties of the vulcanizates before and after thermal aging were evaluated.

RESULTS AND DISCUSION

Cure characteristics

The cure characteristics, expressed in terms of scorch time, optimum cure time, torque values, and cure rate index are reported in Table II, respectively.

The minimum torque (ML) in the rheograph gives an indication of the initial viscosity before crosslinking while the maximum torque (MH) is a measure of crosslink density and stiffness in the rubber.[4] Minimum and maximum torques increased successively with the organoclay content, as shown in Table II. The presence of organoclay generated an increase in the viscosity of the mixtures and, consequently, an increase in ML. The minimum torque value got almost double for the composite prepared with 15 phr organoclay. The increment in MH has a direct relation with the modulus of the vulcanizate.[5] Filler particles dispersed in SBR matrix restrict the mobility of SBR macromolecular chains and consequently, the maximum torque increases with the filler loading.[6]

TABLE II
Curing Characteristics of SBR Nanocomposites

Clay (phr)	ML (dNm)	MH (dNm)	MH-ML (dNm)	t_{97} (min)	ts_2 (min)	CRI (min^{-1})
0	0.54	8.53	7.99	67.31	5.27	1.56
2.5	0.67	9.48	8.81	57.25	6.78	1.98
5	0.69	9.77	9.08	52.74	6.61	2.17
10	0.86	10.44	9.58	54.97	5.94	2.04
15	1.00	11.73	10.73	49.61	5.81	2.23

ML, minimum torque; MH, Maximum torque; t_{97}, Optimum Cure time; ts_2, Scorch time; CRI, Cure Rate index.

The values of torque difference (ΔT = MH-ML) increased as the amount of organoclay increased. The ΔT reflects the crosslink density since it begins to increase from the minimum torque point by crosslinking reactions and the increment in ΔT is due to the reinforcing effect by filler.[7,8]

The addition of organoclay to the SBR accelerated the cure kinetics as observed by the reduction of the optimum cure time (t_{97}). This effect was proportional to the amount of the organoclay added being maximum at 15 phr. The t_{97} dropped down 10 min when only 2.5 phr of organoclay were added, and it was reduced further at higher loadings. A decrease close to 17 min was observed for compounds containing 15 phr of organoclay. The cure activation of organoclays is previously reported in the literature.[9–15] This effect was attributed to the ammonium groups present in the nanosilicate structure. These modifiers take part in amine complexation reaction (like an accelerator), which will accelerate the vulcanization reaction and hence there is a reduction in cure time.

The scorch time (ts_2) is defined as the time up to the onset of vulcanization or crosslinking in rubber compounds. The addition of organoclay produced a little effect on the scorch time of the compounds. ts_2 values were slightly higher in the filled vulcanizates than the unfilled SBR, perhaps because the adsorption of curatives on the filler surface at the beginning of curing.[16] A gradual decrease in ts_2 with the increasing organoclay loading was observed.

The cure rate index (CRI), which indicates the rate of cure of the compounds, was defined as $100/(t_{97}\text{-}ts_2)$. A higher value of CRI means a higher rate of vulcanization. The incorporation of organoclay accelerated the vulcanization process and the curing rate increased with filler content.

Structure characterization

XRD is widely used to understand whether a true nanocomposite has been formed or not. Appearance

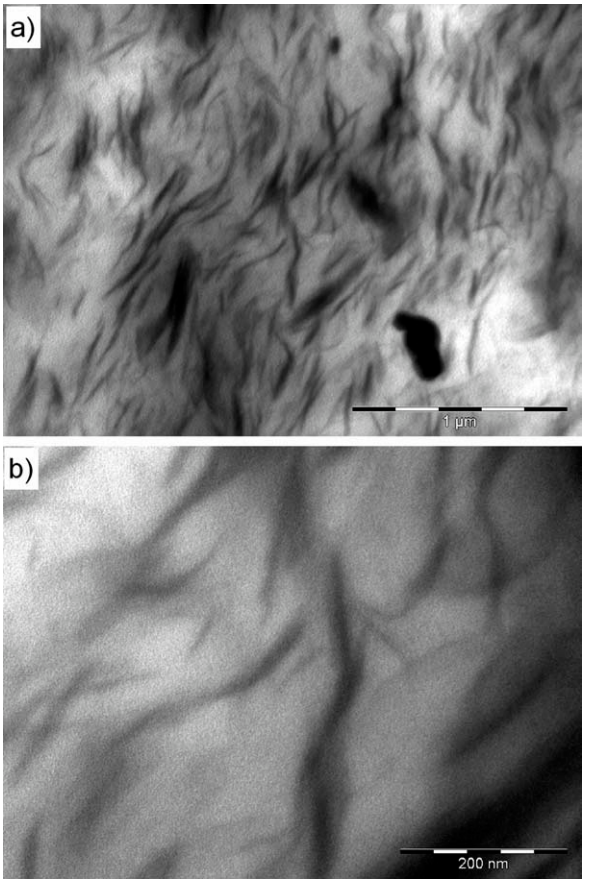

Figure 2 TEM images of the SBR nanocomposite filled with 15 phr organoclay at various magnifications.

of peak at lower angle corresponding to higher interlayer distance indicating intercalated nanocomposites. Based on the XRD patterns the distance between the layers of the organoclay used was 2.2 nm. This was calculated from the related peak at $2\theta = 4.3^\circ$ by the Bragg's law. The addition of organoclay shifted the peak toward lower angles. As a representative example, the SBR with 15 phr organoclay showed a peak at $2\theta = 2.2^\circ$, corresponding to interlayer distance of 3.9 nm, demonstrating thus the existence of intercalated nanocomposites.

Figure 2 shows the dispersed structure of organoclay in the nanocomposite with 15 phr organoclay. The dark lines or areas in the figure correspond to the clay platelets dispersed in the SBR matrix at the nano level. The thickness of most silicate platelets is about 10–20 nm and the length is about 200–300 nm. Even though XRD indicated all intercalated structures, exfoliated layers can also be observed in the TEM pictures [Fig. 2(b)]. Large silicate aggregates and intercalated/exfoliated platelets are simultaneously present.

Mechanical properties of SBR/organoclay nanocomposites

The effect of organoclay on the mechanical properties of SBR composites was analyzed, and the results are summarized in Table III. The tensile strength of the composites increased linearly with the filler loading ($r = 0.9926$). Three-fold increase in tensile strength was obtained for the composite with 15 phr of organoclay. This improvement in tensile strength can be explained by the dispersion of the silicate in the SBR matrix and the increased crosslink density.[8,15] The reinforcing effect is estimated according to the values of the modulus at 100% elongation, M100, which is also an indicator of the stiffness of the rubbers. Note that M100 augmented slightly with organoclay filler and the maximum enhancement was shown at 15 phr loading.

Further, the elongation at break of the vulcanizates increased with organoclay loading. In particular, a 270% increase was obtained for the composites with 15 phr of organoclay.

High tensile strength values are usually associated with lower elongation values; the reinforcing efficiency of organoclay and the increase of crosslinking degree should be accompanied a reduction in elongation at break. Cataldo[17] reported a gradual reduction in elongation at break values in nanoclay filled rubbers, consequence of the stiffening effect exerted by the nanoclay added. In this work, organocomposites showed high tensile strength along with high elongation. This may be explained by intercalated/exfoliated structure of the organoclay filled SBR vulcanizates, which allows silicate layers orient along the direction of stress and contribute to increase tensile strength and elongation at break. The increase of chemical and physical crosslink, the slippage of polymer molecules on the surface of silicate layers

TABLE III
Mechanical Properties of SBR Organocomposites

Clay (phr)	Elongation at break (%)	Tensile strength (MPa)	M100 (MPa)	Tear strength (kN/m)	Compression set (%)	Rebound resilience (%)	Hardness shore A
0	189 ± 9	1.76 ± 0.08	1.12 ± 0.05	8.04 ± 0.97	9.3 ± 1.2	67.5 ± 1.0	44.5 ± 0.8
2.5	209 ± 16	2.09 ± 0.17	1.30 ± 0.10	10.12 ± 0.76	13.2 ± 0.5	66.3 ± 0.5	48.9 ± 0.5
5	348 ± 38	2.85 ± 0.32	1.31 ± 0.06	13.47 ± 0.49	14.2 ± 0.2	65.2 ± 1.8	49.9 ± 0.7
10	434 ± 28	4.12 ± 0.22	1.59 ± 0.09	17.93 ± 0.56	16.3 ± 0.2	63.8 ± 0.3	54.2 ± 0.5
15	516 ± 50	5.97 ± 0.64	2.11 ± 0.19	24.45 ± 1.24	19.9 ± 0.5	58.0 ± 0.7	60.4 ± 0.9

TABLE IV
Glass Transition Temperature and Storage Modulus at 25°C Values for SBR/Organoclay Nanocomposites

Clay loading (phr)	T_g (°C)	Storage modulus (Pa), 25°C
0	−32.9	6.9×10^5
2.5	−34.6	8.1×10^5
5	−34.4	9.3×10^5
10	−33.5	1.1×10^6
15	−33.8	1.0×10^6

and between silicate layers may also cause the increase of elongation.[8,11,15,18]

The values of tear strength, a measure of resistance to crack propagation, are given in Table III. It is observed that the tear strength increased linearly with the organoclay loading ($r = 0.9973$). A 300% increase was observed at 15 phr loading in comparison with unfilled SBR. This effect may be assigned to the dispersion of organoclay at nanometer level and the high interfacial action between the layers and the rubber. The dispersed silicate layers may divert the tear path, which in turn imparts high tear strength to nanocomposites.[11,19]

The ability for the SBR vulcanizates to recover after being under constant deflection was evaluated through compression set and resilience behavior. A clear increase of the compression set with organoclay content was observed being maximum at 15 phr organoclay. On the contrary, the rebound resilience decreased with the filler content.

Organoclay addition gave a higher hysteresis due to the increment in polymer-filler friction and the dislodging of polymer segments from filler surfaces, and this improved the damping gum.

Generally, a decrease in compression set and an increase in resilience indicate a good elastic property of rubber.[11,20] In this work, these results suggested that the elasticity of the SBR vulcanizates decreased slightly with addition of organoclay.

Increase organoclay loading in the rubber matrix resulted in stiffer and harder composites. Shore A hardness passed from a value of 44.5 in the unfilled rubber to 48.9 at 2.5 phr nanoclay and to 60.4 at 15 phr nanoclay loading. This increment was nearly representing a linear relationship ($r = 0.9897$). It is clear that filled vulcanizates had higher hardness compared with unfilled vulcanizates. This enhancement was related with a higher strength of the composites and would reduce the resilience, in concordance with the results obtained.

Dynamic mechanical properties

The glass transition temperature (T_g) was determined as the peak maximum position of the loss factor (tan δ) versus temperature. The addition of organoclay did not significantly change the T_g values from unfilled rubber, as shown in Table IV. However, the intensity of the tan δ peak at the glass transition temperature decreased with increasing the clay content (Fig. 3). This decrease is due to the stronger interaction between SBR and organoclay[21,22] indicating a higher reinforcing efficiency.[23,24] Reduced chain mobility owing to physical and chemical adsorption of the rubber molecules on the filler surface causes a height reduction of tan δ peak during dynamic mechanical deformation.[24] The tan δ values for SBR nanocomposites containing 10 phr and 15 phr organoclay showed a slight increase at temperatures higher than 40°C. This behavior can be explained as filler network relaxation process that could be due to a thermally induced transition for long alkylamonium chains of organoclay.[21,25]

The storage modulus in the rubbery region (0–70°C) of SBR/organoclay nanocomposites was higher than that of unfilled SBR, and tended to increase with increasing organoclay content up to 10 phr and then became constant. This fact reflects the confinement of rubber in the silicate layers.[26] As a representative value, the storage modulus data at 25°C are presented in Table IV.

Thermal decomposition

In Figure 4, the thermogravimetric analysis of organically modified clay revealed several steps linked to a volatile departure. The low temperature step, below 200°C, is associated to the vaporization of free water and water bonded to the cations by hydrogen bonds.[27]

The organic component was evolved in two steps in the temperature range between 200 and 445°C. The first event of decomposition, that is in

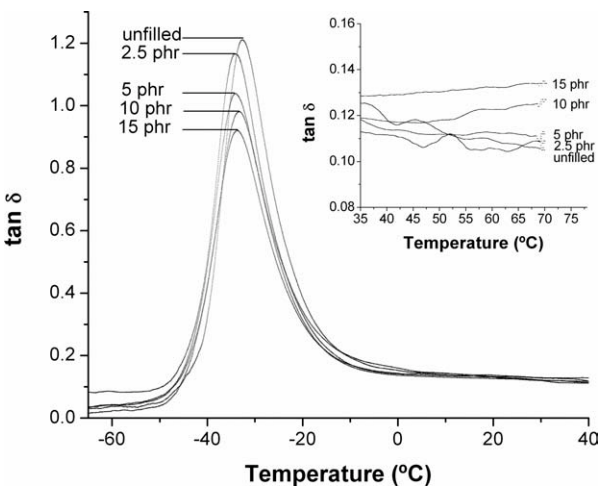

Figure 3 tan δ versus temperature plot of SBR/organoclay nanocomposites.

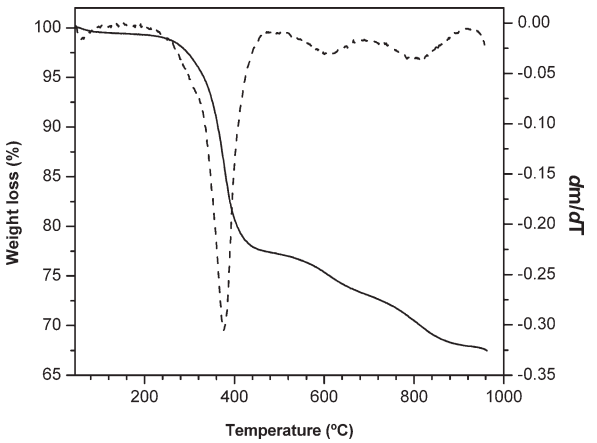

Figure 4 Thermogravimetric curves (–) and derivative thermogravimetric curves (--) of organophilic montmorillonite.

correspondence with the shoulder at about 300°C, is due to the decomposition of the octadecylammonium ions that are weakly linked to the clay surfaces: either complexed outside the interlamellar galleries or inside the interlayers but in a peripheral position.[28] The well intercalated octadecylamonium ions show higher thermal stability and the decomposition takes place at temperatures around 375°C.

The dehydroxylation of the montmorillonite layers took place at temperature between 530 and 675°C. At higher temperatures, the weight loss was ascribed to the evolution of carbonaceous residues. The total weight loss of the organoclay was about 33%.

Thermal properties of SBR vulcanizates are shown in Figure 5. SBR unfilled showed good thermal stability, with an initial temperature of weight loss at approximately 400°C. One decomposition step of thermal degradation was observed, with the temperature of the maximum degradation rate (DTG_{max}) about 460°C. For SBR filled composites, the presence of organoclay did not significantly shift the onset of decomposition. However, the filler contributed to a broader degradation process, with a remarkably increase in DTG_{max} values compared to SBR unfilled, which indicated a slight stabilizing effect. An increase in DTG_{max} with up to 10 phr of organoclay content was observed. A further decrease was observed at higher clay loading.

This trend was similar to that recorder in the temperature at which 50% degradation occurs (T_{50}). In particular, T_{50} value increased 12°C in relation to unfilled rubber when only 2.5 phr organoclay were added.

The improvement in thermal stability could be related to the uniform dispersion of organoclay[29] because of the nanoparticles between the chains of rubber prevents diffusion of volatile decomposition products.[30] The enhanced char yield was observed in the high temperature region with increasing organoclay content, and the char residue formation usually governed the flammability behavior of nanostructured materials.[26]

Thermal aging resistance

Elastomers degrade in a variety of environments and service conditions limiting their service lifetime. Oxidative degradation is generally considered to be the most serious problem in the use of rubber at high temperature. During thermal aging, main-chain scission, crosslink formation and crosslink breakage can occur. The change in properties of polymers on aging depends on the extent of such reactions. There have been several methods developed to monitor the aging conditions of rubber. Tensile strength,

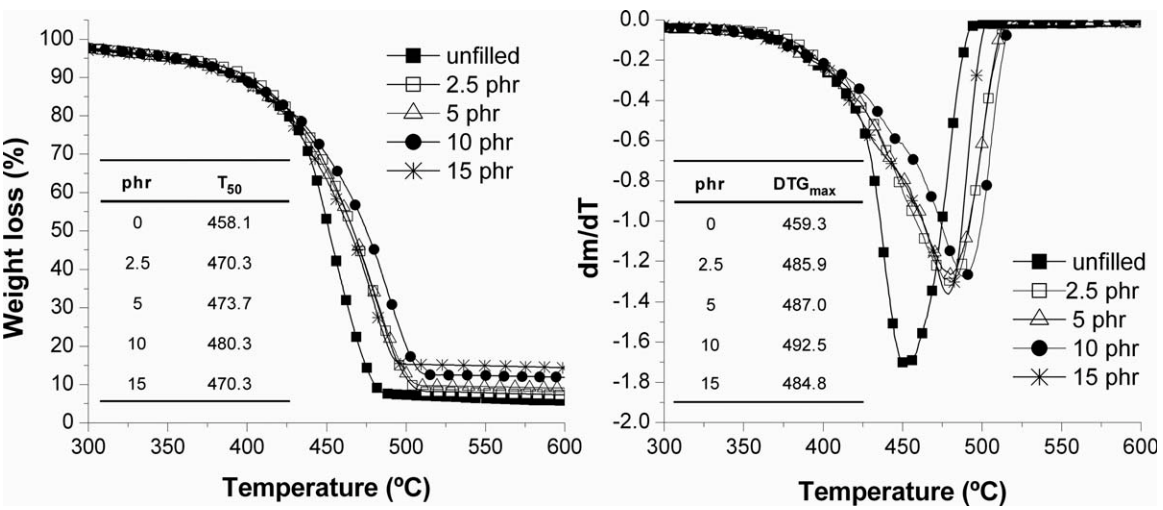

Figure 5 Thermogravimetric curves (a) and derivative thermogravimetric curves (b) of unfilled SBR and SBR/organoclay nanocomposites.

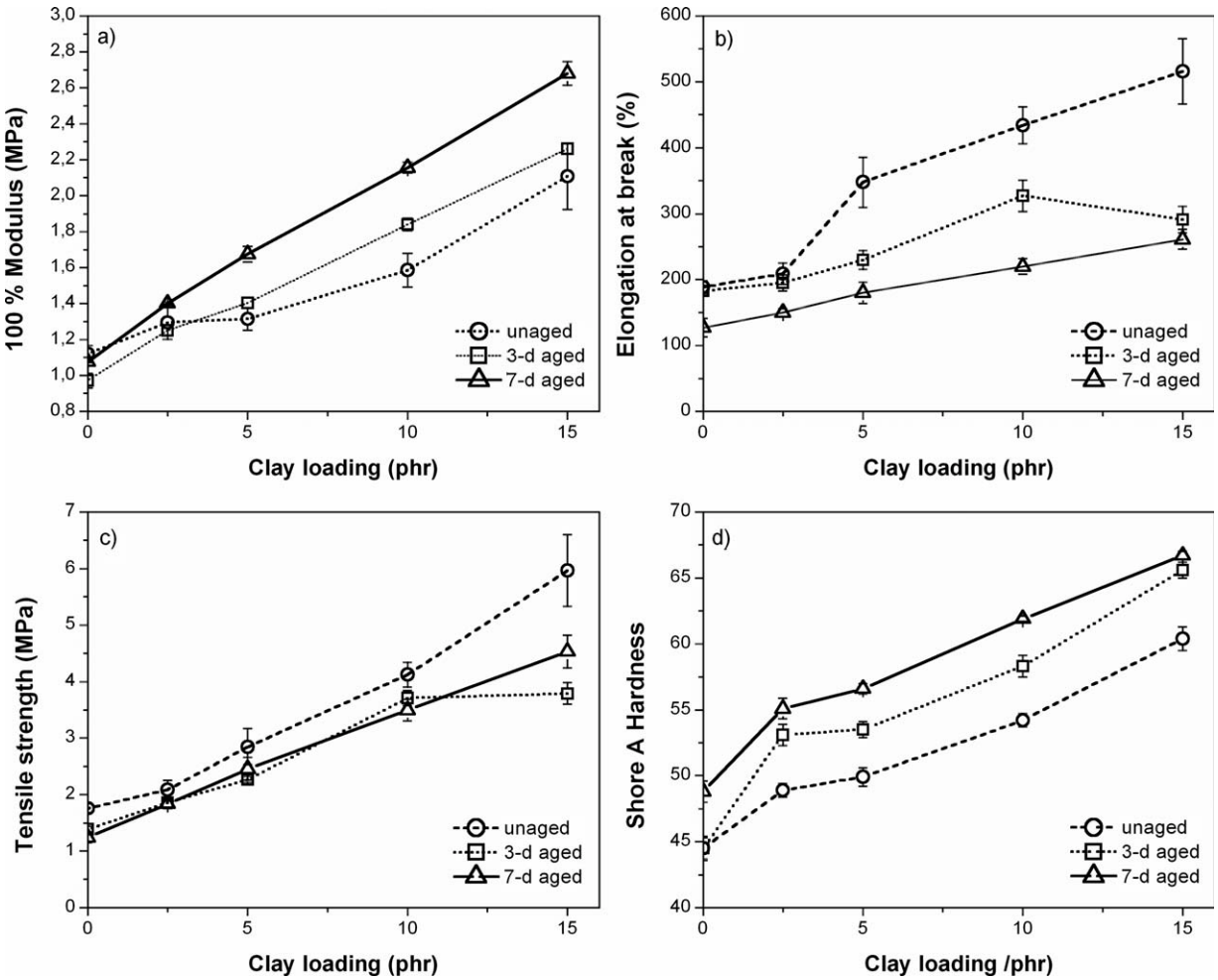

Figure 6 Effect of thermal aging on the modulus at 100% elongation (M100) (a), elongation at break (b), tensile strength (c), and hardness (d) of organoclay filled SBR vulcanizates.

elongation at break and hardness testing are often found to be useful indicators of the remaining mechanical properties.[31,32]

Figures 6(a–c) show the tensile properties of SBR filled vulcanizates before and after thermal aging. The modulus at 100% elongation after thermal aging was higher than before thermal aging when organoclay content was higher than 5 phr. This is may attributed to the formation of additional crosslinks.[33] The increase in crosslinks reduces the mobility of rubber chains and, as consequence, a reduction in elongation at break was observed for all aged samples. As expected, at the same filler loading, the lowest elongation at break was observed at longer times of aging.

The tensile strength at break also decreased after thermal aging. This may be because the degree of crosslinking after aging exceeds an optimum value and the networks become too dense, leading to the decrease in tensile strength while the moduli increase.[32]

Figure 6(d) shows the variation of hardness versus aging time for SBR with different organoclay loading. It is clear that for each formulation the hardness value increased as aging time increased. This is probably due to the crosslink formation and the oxidizing skin, which results from the oxygen uptake at the surface of the specimen.[24,31,34]

CONCLUSIONS

The following conclusions were derived from the experimental results:

1. The presence of organoclay decreased the cure time of the vulcanizates, which decreased with the amount of filler added. This effect was attributed to the ammonium groups present in the organoclay structure that acts accelerating the vulcanization reaction. The torque difference of the SBR/organoclay composites was found sensibly higher than the unfilled SBR and increased as the amount of organoclay increased, suggesting a higher crosslink density.

2. All values in mechanical properties except rebound resilience increased with the increase of organoclay. The enhancement of the mechanical properties could be considered from uniform dispersion of clay in the rubber matrix and the planar orientation of the organoclay layers.
3. The intensity of the tan δ peak decreased with increasing the clay content, suggesting a higher reinforcing efficiency. However, the addition of organoclay had negligible effect on the glass transition temperature. The storage modulus of the vulcanizates in the rubbery plateau tended to increase with increasing organoclay loading, reflecting the strong confinement of organoclay layers on the rubber chains.
4. The addition of organoclay improved the thermal stability of the vulcanizates, as shown DTG_{max} and T_{50} values, probably due that the nanoparticles between the chains of rubber prevents the diffusion of the volatile decomposition products.
5. Due to thermal aging both the elongation at break and tensile strength for SBR/organoclay vulcanizates decreased. This may be due to the crosslink formation in a post-curing step and to the oxidative degradation. This phenomenon was more pronounced at longer aging times. On the contrary, the values of the modulus at 100% elongation were found to increase upon aging.

References

1. Sadhu, S. D.; Maiti, M.; Bhowmick, A. K. In Current Topics in Elastomers Research; Bhowmick, A. K., Ed.; CRC Press: Boca Raton, Florida, 2008; Chapter 2.
2. Mohammad, A.; Simon, G. P. Polymer Nanocomposites; Mai, W.-Y., Yu, Z.-Z., Eds.; Woodhead Publishing Limited: Cambridge, 2006; Chapter 12.
3. Sengupta, R.; Chakraborty, S.; Bandyopadhyay, S.; Dasgupta, S.; Mukhopadhyay, A. K.; Deuri, A. S. Polym Eng Sci 2007, 47, 1956.
4. Jacob, M.; Thomas, S.; Varghese, K. T. Compos Sci Technol 2004, 64, 955.
5. Jacob, A.; Kurian, P.; Aprem, A. S. Int J Polym Mater 2007, 56, 593.
6. Tan, H.; Isayev, A. J Appl Polym Sci 2008, 109, 767.
7. Jeon, H. U.; Lee, D. H.; Choi, D.-J.; Kim, M. S.; Kim, J. H.; Jeong, H. M. J Macromol Sci Phys 2007, 46, 1151.
8. Choi, S.-S.; Park, B.-H.; Song, H. Polym Adv Technol 2004, 15, 122.
9. Hrachová, J.; Komadel, P.; Chodák, I. J Mater Sci 2008, 43, 2012.
10. Arroyo, M.; López-Manchado, M. A.; Valentín, J. L.; Carretero, J. Compos Sci Technol 2007, 67, 1330.
11. Madhusoodanan, K. N.; Varghese, S. J Appl Polym Sci 2006, 102, 2537.
12. Varghese, S.; Karger-Kocsis, J. J Appl Polym Sci 2004, 91, 813.
13. Teh, P. L.; Mohd Ishak, Z. A.; Hashim, A. S.; Karger-Kocsis, J.; Ishiaku, U. S. J Appl Polym Sci 2004, 94, 2438.
14. Song, M.; Wong, C. W.; Jin, J.; Ansarifar, A.; Zhang, Z. Y.; Richardson, M. Polym Int 2005, 54, 560.
15. Mousa, A.; Karger-Kocsis, J. Macromol Mater Eng 2001, 286, 260.
16. Gu, Z.; Song, G.; Liu, W.; Li, P.; Gao, L.; Li, H.; Hu, X. Appl Clay Sci 2009, 46, 241.
17. Cataldo, F. Macromol Symp 2007, 247, 67.
18. Mousa, A. Int J Polym Mater 2007, 56, 355.
19. Chang, Y.-W.; Yang, Y.; Ryu, S.; Nah, C. Polym Int 2002, 51, 319.
20. Sombatsompop, N.; Wimolmala, E.; Markpin, T. J Appl Polym Sci 2007, 104, 3396.
21. Schön, F.; Thomann, R.; Gronski, W. Macromol Symp 2002, 189, 105.
22. Praveen, S.; Chattopadhyay, P. K.; Albert, P.; Dalvi, V. G.; Chakraborty, B. C.; Chattopadhyay, S. Compos A: Appl Sci Manuf 2009, 40, 309.
23. Varghese, S.; Karger-Kocsis, J.; Gatos, K. G. Polymer 2003, 44, 3977.
24. Das, A.; Costa, F. R.; Wagenknecht, U.; Heinrich, G. Eur Polym J 2008, 44, 2456.
25. Lu, Y.-L.; Li, Z.; Yu, Z.-Z.; Tian, M.; Zhang, L.-Q.; Mai, Y.-W. Compos Sci Technol 2007, 67, 2903.
26. Abdollahi, M.; Rahmatpour, A.; Aalaie, J.; Khanli, H. H. e-Polymers 2007, 74.
27. Xie, W.; Gao, Z.; Liu, K.; Pan, W.-P.; Vaia, R.; Hunter, D.; Singh, A. Thermochim Acta 2001, 367, 339.
28. Bellucci, F.; Camino, G.; Frache, A.; Sarra, A. Polym Degrad Stab 2007, 92, 425.
29. Mishra, S.; Shimpi, N. G.; Patil, U. D. J Polym Res 2007, 14, 449.
30. Zhang, H.; Wang, Y.; Wu, Y.; Zhang, L.; Yang, J. J Appl Polym Sci 2005, 97, 844.
31. Mostafa, A.; Abouel-Kasem, A.; Bayoumi, M. R.; El-Sebaie, M. G. Mater Des 2009, 30, 791.
32. Sadhu, S.; Bhowmick, A. K. J Appl Polym Sci 2004, 92, 698.
33. Rattanasom, N.; Prasertsri, S. Polym test 2009, 28, 270.
34. Tian, M.; Cheng, L.; Liang, W.; Zhang, L. J Appl Polym Sci 2006, 101, 2725.